JOURNAL OF BACTERIOLOGY, Apr. 2009, p. 2012–2022 Vol. 191, No. 7
0021-9193/09/$08.00+0 doi:10.1128/JB.01547-08

Mutations in *ampG* and Lytic Transglycosylase Genes Affect the Net Release of Peptidoglycan Monomers from *Vibrio fischeri*▽†

Dawn M. Adin,[1] Jacquelyn T. Engle,[2] William E. Goldman,[2,3] Margaret J. McFall-Ngai,[4] and Eric V. Stabb[1]*

Department of Microbiology, University of Georgia, Athens, Georgia 30605[1]; Department of Molecular Microbiology, Washington University, St. Louis, Missouri 63110[2]; Department of Microbiology and Immunology, University of North Carolina, Chapel Hill, North Carolina 27517[3]; and Department of Medical Microbiology and Immunology, University of Wisconsin, Madison, Wisconsin 53706[4]

Received 31 October 2008/Accepted 5 December 2008

The light-organ symbiont *Vibrio fischeri* releases *N*-acetylglucosaminyl-1,6-anhydro-*N*-acetylmuramylalanyl-γ-glutamyldiaminopimelylalanine, a disaccharide-tetrapeptide component of peptidoglycan that is referred to here as "PG monomer." In contrast, most gram-negative bacteria recycle PG monomer efficiently, and it does not accumulate extracellularly. PG monomer can stimulate normal light-organ morphogenesis in the host squid *Euprymna scolopes*, resulting in regression of ciliated appendages similar to that triggered by infection with *V. fischeri*. We examined whether the net release of PG monomers by *V. fischeri* resulted from lytic transglycosylase activity or from defects in AmpG, the permease through which PG monomers enter the cytoplasm for recycling. An *ampG* mutant displayed a 100-fold increase in net PG monomer release, indicating that AmpG is functional. The *ampG* mutation also conferred the uncharacteristic ability to induce light-organ morphogenesis even when placed in a nonmotile *flaJ* mutant that cannot infect the light-organ crypts. We targeted five potential lytic transglycosylase genes singly and in specific combinations to assess their role in PG monomer release. Combinations of mutations in *ltgA*, *ltgD*, and *ltgY* decreased net PG monomer release, and a triple mutant lacking all three of these genes had little to no accumulation of PG monomers in culture supernatants. This mutant colonized the host as well as the wild type did; however, the mutant-infected squid were more prone to later superinfection by a second *V. fischeri* strain. We propose that the lack of PG monomer release by this mutant results in less regression of the infection-promoting ciliated appendages, leading to this propensity for superinfection.

Microbe-associated molecular patterns (MAMPs) are recognized by hosts in a variety of pathogenic and symbiotic relationships. MAMP is an umbrella term for a variety of semiconserved bacterial molecules, including lipopolysaccharide, lipoproteins, flagella, and peptidoglycan (PG), that are sensed by conserved host surveillance mechanisms (e.g., the innate immune system), triggering context-dependent reactions to bacterial colonization. Mounting evidence shows that PG-derived MAMPs play important and previously underappreciated roles in host-bacterium interactions (11).

The PG layer of gram-negative bacteria is a rigid network in the periplasm that protects against osmotic lysis and helps to determine cell size and shape while still allowing diffusion of molecules into the cell (14). In PG, repeated subunits of *N*-acetylglucosamine and *N*-acetylmuramic acid are connected to a short pentapeptide side chain of L-alanyl-D-γ-glutamyl-*meso*-diaminopimelyl-D-alanyl-D-alanine (Ala-Glu-DAP-Ala-Ala). Adjacent peptides are cross-linked through Ala-DAP or DAP-DAP peptide bonds, and side chains are converted to tetra-, tri-, and dipeptides through the action of carboxypeptidases in the periplasm (19, 49).

Despite its mechanical stability, PG is a dynamic structure that undergoes remodeling and recycling. Murein hydrolases, including lytic transglycosylases, hydrolyze PG to allow the insertion of new material as the cell grows or to accommodate structures that span the periplasm (61, 72). Lytic transglycosylases cleave the *N*-acetylmuramic acid-β-1,4-*N*-acetylglucosamine linkage in PG and catalyze the formation of a 1,6-anhydro bond on the *N*-acetylmuramic acid (28). After cleavage, PG monomers enter the cytoplasm through the permease AmpG (30) and are recycled and ultimately reincorporated into PG (20). Murein hydrolase activity and the recycling of PG monomers presumably allow for growth and cell expansion; however, *Escherichia coli* mutants lacking *ampG* or several lytic transglycosylases were not affected in growth or cell division (25, 33).

Presumably because PG monomers are usually efficiently recycled, only a few bacteria are known to release PG monomers during growth. These include *Neisseria gonorrhoeae* (62) and *Bordetella pertussis* (57), which cause gonorrhea and whooping cough, respectively. These pathogens each release *N*-acetylglucosaminyl-1,6-anhydro-*N*-acetylmuramylalanyl-γ-glutamyldiaminopimelylalanine (referred to herein as "PG monomer"), which triggers the death of ciliated host cells (12, 38, 42), but the basis for their shedding of PG monomers differs. *B. pertussis* release of PG monomer, or "tracheal cytotoxin" (TCT), apparently is due to disruption of *ampG* expression by the insertion of an IS*481* element 90 bp upstream of this gene (36), and artificially expressing *ampG* in *B. pertussis*

* Corresponding author. Mailing address: University of Georgia, Department of Microbiology, 1000 Cedar Street, Athens, GA 30602. Phone: (706) 542-2414. Fax: (706) 542-2674. E-mail: estabb@uga.edu.

† Supplemental material for this article may be found at http://jb.asm.org/.

▽ Published ahead of print on 12 December 2008.

decreased PG monomer release (36, 43). However, in *N. gonorrhoeae* the activities of the lytic transglycosylases LtgA (9) and LtgD (10) appear to be responsible for the release of PG monomer or "PG cytotoxin" (PGCT). An *ampG* mutant in *N. gonorrhoeae* showed a sevenfold increase in PG monomer release, suggesting a functional AmpG and PG recycling pathway (18). Unfortunately, humans are the host for *N. gonorrhoeae* and *B. pertussis*, hindering examination of the effects of PG monomer during natural infections.

Recently, the bioluminescent marine bacterium *Vibrio fischeri* was found to release the same PG monomer as that released by *N. gonorrhoeae* and *B. pertussis* (31). *V. fischeri* is a light-organ symbiont of the Hawaiian bobtail squid, *Euprymna scolopes*, and this host-bacterium association can be reconstituted in the laboratory. *E. scolopes* hatchlings contain ciliated appendages that increase water flow across the light organ and help facilitate infection (40, 41, 48). During initial colonization, *V. fischeri* triggers regression of these ciliated fields (15, 47), and this can be mimicked by adding PG monomers to the seawater (31). In this study, we constructed and analyzed mutants to determine the contributions of lytic transglycosylases and AmpG to PG monomer release in *V. fischeri*. We also determined the abilities of the mutants to colonize and stimulate morphogenesis of the squid host.

MATERIALS AND METHODS

Bacterial strains, plasmids, and growth conditions. The strains used in this study are listed in Table 1. *E. coli* was incubated at 37°C in LB medium (44), brain heart infusion medium (Difco, Sparks, MD), or, for PG monomer analysis, M9 minimal medium (60) with 30 mM glucose. When added to LB medium (44) for selection of *E. coli*, chloramphenicol (Cm) and kanamycin were used at concentrations of 20 and 40 $\mu g\ ml^{-1}$, respectively. For selection of *E. coli* with erythromycin (Em), 150 $\mu g\ ml^{-1}$ was added to brain heart infusion medium. *V. fischeri* was grown at 28°C in LBS (63) or at 24°C in SWT and SWTO (5) or minimal salts medium (0.340 mM $NaPO_4$ [pH 7.5], 0.05 M Tris [pH 7.5], 0.3 M NaCl, 0.05 M $MgSO_4 \cdot 7H_2O$, 0.01 M $CaCl_2 \cdot 2H_2O$, 0.01 M NH_4Cl, 0.01 M KCl, 0.01 mM $FeSO_4 \cdot 7H_2O$, and 30 mM glucose). When added to LBS for selection of *V. fischeri*, Cm, kanamycin, and Em were used at concentrations of 2, 100, and 5 $\mu g\ ml^{-1}$, respectively. Agar was added to a final concentration of 1.5% for solid media.

DNA and plasmid manipulations. Standard methods were used to manipulate plasmids and DNA fragments. Plasmids were transformed and maintained in *E. coli* DH5α, except plasmids with the R6K origin of replication or pCR-BluntII TOPO, which were maintained in DH5αλ*pir* and TOP10, respectively. Restriction enzymes and T4 DNA ligase were obtained from New England Biolabs (Ipswich, MA). Chromosomal DNA was purified using the Easy-DNA kit (Invitrogen, Carlsbad, CA). Plasmids were isolated using the QIAprep Spin Miniprep kit (Qiagen, Valencia, CA) or the GenElute Plasmid Miniprep kit (Sigma, St. Louis, MO). The Zero Blunt TOPO PCR cloning kit (Invitrogen, Carlsbad, CA) was used to clone PCR products into pCR-BluntII TOPO. DNA fragments were purified using the DNA Clean & Concentrator-5 kit (Zymo Research, Orange, CA). PCR was performed using KOD HiFi DNA polymerase (Novagen, Madison, WI) by following the manufacturer's recommendations for cycle programs based on predicted product size. The annealing temperature for each primer was usually determined by subtracting 5°C from the lower calculated primer melting temperature. PCR was performed using an iCycler (Bio-Rad Laboratories, Hercules, CA). DNA sequencing was conducted on an ABI automated DNA sequencer at the University of Michigan DNA Sequencing Core, and sequences were analyzed using Sequencher 4.6 (Gene Codes, Ann Arbor, MI). Oligonucleotides (Table 1) were obtained from Integrated DNA Technologies (Coralville, IA).

Mutant construction. Descriptions of select plasmids and the primers used in their construction are provided in Table 1. Construction of mutant strains and alleles is outlined in Table 1, and a summary follows. To generate plasmid insertion mutants, an internal fragment of each targeted gene was PCR amplified and either cloned directly into pEVS122 (a vector that does not replicate in *V. fischeri*) or cloned into pCR-BluntII TOPO and subsequently subcloned into pEVS122. The resulting plasmids were mobilized into *V. fischeri*, and plating on LBS-Em selected for transconjugants that had undergone homologous recombination between the genome and the internal gene fragment, enabling us to isolate vector integration mutants. In this way, plasmids pDMA48, pDMA89, pDMA90, pDMA91, pDMA108, and pDMA109 were used to generate mutations in *ampG*, *ltgA*, *ltgY*, *ltgD*, *lysM*, and *ltgE*, respectively. In-frame Δ*ampG*, Δ*ltgA*, and Δ*ltgD* deletion alleles were constructed in plasmids pDMA110, pDMA187, and pDMA199, respectively, such that the region between the start and stop codon of each target gene was replaced by a 6-bp restriction enzyme recognition site. These in-frame deletion mutations were placed in ES114 or in mutant backgrounds by allelic exchange. All mutants were confirmed by PCR. Constructs were generated in *E. coli* and transferred to *V. fischeri* by triparental mating using *E. coli* CC118λ*pir* pEVS104 as a conjugative helper plasmid (65).

Bioinformatic analyses. Protein sequence comparisons to GenBank entries were generated using BLAST-P (2) and the BLOSUM62 scoring matrix (26). Genomes with similar regions surrounding the lytic transglycosylase open reading frames (ORFs) were found using the SEED pinned region search (54). To assess genetic context within the *Vibrionaceae* family, we compared local gene arrangement in *V. fischeri* ES114 (59) to that in the genomes of *Vibrio alginolyticus* 12G01, *Vibrio angustum* S14, *Vibrio campbellii* AND4, *Vibrio cholerae* O1 biovar eltor strain N16961 (23), *Vibrio harveyi* ATCC BAA-1116, *Vibrio parahaemolyticus* RIMD 2210633 (37), *Vibrio vulnificus* CMCP6 (8), and *Photobacterium profundum* SS9 (69). Sequence alignments were performed with MEGA 4.0 using the default settings (66). The similarity and identity between homologs reported were determined with MatGAT using the default settings (7).

PG monomer detection and quantification. Culture supernatants were subject to solid-phase extraction and reversed-phase high-pressure liquid chromatography (HPLC) as described previously (12, 31). Briefly, cultures were grown in minimal medium supplemented with 30 mM glucose at 24°C until reaching an optical density at 595 nm (OD_{595}) of ~0.8 to 1.0 (mid- to late-log growth). Cultures were centrifuged either in 15-ml Falcon tubes (two spins at 4,500 × *g* for 10 min each at 4°C) or by sequential spins in a 250-ml centrifuge bottle at 4,500 × *g* and then in a 30-ml centrifuge bottle at 8,500 × *g*, each for 10 min at 4°C, to pellet cells. Culture supernatants were adjusted to 1% trifluoracetic acid (TFA) with 100% TFA and filtered through an 0.22-μm mixed cellulose membrane filter unit (Fisher Scientific, Hanover Park, IL). Each sample was desalted using a C_{18} Plus Sep-Pak cartridge (Waters Corporation, Milford, MA), and each cartridge was prepared prior to receiving the sample with 100% methanol and two washes with 0.1% TFA in water. Samples were then loaded and allowed to flow by gravity through the column. After complete loading, the column was washed twice with 10 ml of 0.1% TFA in water. Materials retained in the column were eluted with 4 ml of 100% methanol and concentrated to dryness under a vacuum with a SpeedVac Plus (ThermoSavant, Holbrook, NY). Two hundred microliters of drying reagent (2 parts H_2O to 2 parts methanol to 1 part triethylamine acetate [TEA]) was added to the dried C_{18} fraction, vortexed, and dried under vacuum in a SpeedVac Plus. Thirty microliters of phenylisothiocyanate (Pierce, Rockford, IL) reagent (10% H_2O, 75% methanol, 10% TEA, and 5% phenylisothiocyanate) was added to derivatize each sample, and the resulting phenylthiocarbamyl (PTC) derivatives were then dried.

Reversed-phase HPLC was employed to separate the PTC-PG monomers from the extract. Buffer A consisted of 150 mM sodium acetate and 0.05% TEA brought to pH 6.35 with glacial acetic acid, and buffer B consisted of a 60:40 mix of acetonitrile and water. Samples were resuspended in a 92:8 solution of buffer A and buffer B such that it was 100-fold more concentrated than culture supernatant. Each sample was vortexed, and 200 μl was injected into the HPLC. A Brownlee Spheri-5, RP-8 C_8 4.6- × 220-mm column with a 4.6- × 30-mm guard column of the same matrix was used for all chromatographic separations (Perkin-Elmer, Waltham, MA). Column temperature was maintained at 35°C with a flow rate of 1 ml/min. The gradient (ratio of buffer A to buffer B) was as follows: 0 min, 92:8; 13 min, 65:35; 15 min, 0:100; 35 min, 0:100; and 36 min, 92:8, with reinjection at 45 min. Absorption at 254 nm was detected using a Spectraflow 757 variable-λ UV detector. Peak areas and retention times were recorded using Dynamic MacIntegration software, version 1.4.1 or 1.4.3. PTC-PG monomer retention time was approximately 13.2 min. A PG monomer standard (*B. pertussis* TCT) was also phenylisothiocyanate derivatized and run to compute picomoles of PG monomer in each sample based on comparisons of peak areas. For experiments assessing PG monomer released by mutant strains, PG monomer releases from wild-type *V. fischeri* ES114 and *E. coli* MG1655 were run as controls. Over 14 different experiments, *V. fischeri* ES114 samples averaged 21.2 ± 3.9 (standard error) nM PG monomer per OD_{595}. As a negative control, *E. coli* MG1655 was included in six experiments and averaged 2.9 ± 1.6 (standard error) nM PG monomer per OD_{595}, with PG monomer being below the limit of detection (~1.5 nM per OD_{595}) in three of these experiments.

TABLE 1. Bacterial strains, plasmids, and oligonucleotides

Strain, plasmid, or oligonucleotide	Relevant characteristics[a,b]	Source or reference
Bacterial strains		
E. coli		
CC118λ*pir*	Δ(*ara-leu*) *araD* Δ*lac74 galE galK phoA20 thi-1 rpsE rpsB argE*(Am) *recA* λ*pir*	27
DH5α	F$^-$ ϕ80d*lacZ*Δ(*lacZYA-argF*)*U169 deoR supE44 hsdR17 recA1 endA1 gyrA96 thi-1 relA1*	22
DH5αλ*pir*	DH5α lysogenized with λ*pir*	16
MG1655	F$^-$ λ$^-$ *ilvG rfb50 rph1*	C. Gross
TOP10	F$^-$ *mcrA* Δ(*mrr-hsdRMS-mcrBC*) ϕ80*lacZ*ΔM15 Δ*lacX74 recA1 ara*Δ*139* Δ(*ara-leu*)*7697 galU galK rpsL* (Str^r) *endA1 nupG*	Invitrogen
V. fischeri		
AKD200	ES114 mini-Tn*7* insertion; Cm^r	A. Dunn
DM131	ES114 *flaJ*::*aph*; Kn^r	D. Millikan
DMA350	ES114 *ampG*::pDMA48; Em^r	This study
DMA352	ES114 Δ*ampG* (allele exchanged from pDMA110 into ES114)	This study
DMA354	DM131 Δ*ampG* (allele exchanged from pDMA110 into ES114); Kn^r	This study
DMA360	ES114 *ltgA*::pDMA89; Em^r	This study
DMA361	ES114 *ltgY*::pDMA90; Em^r	This study
DMA362	ES114 *ltgD*::pDMA91; Em^r	This study
DMA363	ES114 Δ*ltgA* (allele exchanged from pDMA187 into ES114)	This study
DMA368	ES114 Δ*ltgD* (allele exchanged from pDMA199 into ES114)	This study
DMA369	ES114 Δ*ltgA* Δ*ltgD* (allele exchanged from pDMA199 into DMA363)	This study
DMA380	ES114 *ltgE*::pDMA109; Em^r	This study
DMA385	ES114 *lysM*::pDMA108; Em^r	This study
DMA386	ES114 Δ*ltgA ltgY*::pDMA90; Em^r	This study
DMA387	ES114 Δ*ltgD ltgY*::pDMA90; Em^r	This study
DMA388	ES114 Δ*ltgA* Δ*ltgD ltgY*::pDMA90; Em^r	This study
ES114	Wild-type isolate from *E. scolopes*	3
Plasmids		
pCR-BluntII TOPO	TOPO PCR cloning vector; Kn^r	Invitrogen
pDMA46	Internal *ampG* fragment (PCR product; primers dma30 and dma31, ES114 template) in pCR-BluntII TOPO; Kn^r	This study
pDMA48	pDMA46 BamHI fragment in BamHI-digested pEVS122; internal *ampG* fragment *ori*$V_{R6K\gamma}$ *ori*T_{RP4} Em^r	This study
pDMA74	Internal *ltgA* fragment (PCR product; primers dma58 and dma59, ES114 template) in pCR-BluntII TOPO; Kn^r	This study
pDMA75	Internal *ltgY* fragment (PCR product; primers dma60 and dma61, ES114 template) in pCR-BluntII TOPO; Kn^r	This study
pDMA76	Internal *ltgD* fragment (PCR product; primers dma62 and dma63, ES114 template) in pCR-BluntII TOPO; Kn^r	This study
pDMA77	*ampG* complementing fragment (PCR product; primers dma52 and dma53, ES114 template) in pCR-BluntII TOPO; Kn^r	This study
pDMA89	pDMA74 BglII fragment in BamHI-digested pEVS122; internal *ltgA* fragment; *ori*$V_{R6K\gamma}$ *ori*T_{RP4} Em^r	This study
pDMA90	pDMA75 BglII fragment in BamHI-digested pEVS122; internal *ltgY* fragment; *ori*$V_{R6K\gamma}$ *ori*T_{RP4} Em^r	This study
pDMA91	pDMA76 BglII fragment in BamHI-digested pEVS122; internal *ltgD* fragment; *ori*$V_{R6K\gamma}$ *ori*T_{RP4} Em^r	This study
pDMA96	~1.5-kb fragment downstream of *ampG* stop (PCR product; primers 55 and dma57, ES114 template) in SmaI-digested pEVS79; *ori*V_{ColE1} *ori*T_{RP4} Cm^r	This study
pDMA100	~1.5-kb fragment upstream of *ampG* start (PCR product; primers dma54 and dma56, ES114 template) in HpaI-digested pJLB103; *ori*$V_{R6K\gamma}$ Kn^r	This study
pDMA104	Internal *lysM* fragment (PCR product; primers dma76 and dma77, ES114 template) in pCR-BluntII TOPO; Kn^r	This study
pDMA105	pDMA96 SmaI digested fused to SmaI-digested pDMA100; *ori*V_{ColE1} *ori*$V_{R6K\gamma}$ *ori*T_{RP4} Kn^r Cm^r	This study
pDMA106	pDMA77 SpeI-XbaI fragment in SpeI-XbaI-digested pEVS79; *ori*V_{ColE1} *ori*T_{RP4} Cm^r	This study
pDMA108	pDMA104 BglII fragment in BamHI-digested pEVS122; internal *lysM* fragment; *ori*$V_{R6K\gamma}$ *ori*T_{RP4} Em^r	This study
pDMA109	Internal *ltgE* fragment (PCR product; primers dma78 and dma79) BamHI digested in BamHI-digested pEVS122; *ori*$V_{R6K\gamma}$ *ori*T_{RP4} Em^r	This study
pDMA110	pDMA105 AvrII-SpeI digested and self-ligated; Δ*ampG* allele; *ori*V_{ColE1} *ori*T_{RP4} Cm^r	This study
pDMA115	pDMA106 SpeI-XbaI fragment in AvrII-digested pVSV104; *V. fischeri ampG* in shuttle vector pVSV104; *ori*$V_{R6K\gamma}$ *ori*T_{RP4} *ori*V_{pES213} Kn^r	This study
pDMA176	~1.5-kb fragment upstream of *ltgA* start (PCR product; primers dma95 and dma99, ES114 template) in pCR-BluntII TOPO; Kn^r	This study
pDMA177	*ltgA* complementing PCR fragment (primers dma97 and dma98, ES114 template) in pCR-BluntII TOPO	This study
pDMA185	~1.5-kb fragment downstream of *ltgA* stop (PCR product; primers dma96 and dma100, ES114 template) in pCR-BluntII TOPO; Kn^r	This study
pDMA186	pDMA182 XhoI digested and self-ligated; *ori*$V_{R6K\gamma}$ *ori*T_{RP4} Cm^r	This study
pDMA187	pDMA185 SmaI fragment in SmaI-digested pDMA186; Δ*ltgA* allele; *ori*$V_{R6K\gamma}$ *ori*V_{ColE1} *ori*T_{RP4} Cm^r	This study
pDMA191	~1.5-kb fragment downstream of *ltgD* stop (PCR product; primers dma102 and dma106, ES114 template) in pCR-BluntII TOPO; Kn^r	This study
pDMA196	pDMA177 SpeI-XhoI fragment in SpeI-XhoI-digested pVSV107; *ltgA* in shuttle vector pVSV107; *ori*$V_{R6K\gamma}$ *ori*T_{RP4} *ori*V_{pES213} Tp^r *lacZ*α	This study
pDMA197	~1.5-kb fragment upstream of *ltgD* start (PCR product; primers dma105 and dma115, ES114 template) in SmaI-digested pEVS122; *ori*$V_{R6K\gamma}$ *ori*T_{RP4} Em^r	This study
pDMA198	pDMA191 KpnI-XbaI fragment in KpnI-XbaI-digested pEVS79; *ori*V_{ColE1} *ori*T_{RP4} Cm^r	This study
pDMA199	pDMA198 SmaI digested fused to SmaI-digested pDMA197; Δ*ltgD* allele; *ori*V_{ColE1} *ori*$V_{R6K\gamma}$ *ori*T_{RP4} Cm^r Em^r	This study
pEVS79	*ori*V_{ColE1} *ori*T_{RP4} Cm^r	65
pEVS104	*ori*$V_{R6K\gamma}$ *ori*T_{RP4} Kn^r RP4-derived conjugative helper plasmid	65
pEVS118	*ori*$V_{R6K\gamma}$ *ori*T_{RP4} Cm^r	16
pEVS122	*ori*$V_{R6K\gamma}$ *ori*T_{RP4} Em^r *lacZ*α	16
pJLB103	pVSV104 BamHI digested and self-ligated; *ori*$V_{R6K\gamma}$ Kn^r *lacZ*α	This study
pVSV102	*ori*$V_{R6K\gamma}$ *ori*T_{RP4} *ori*V_{pES213} Kn^r *gfp*	17
pVSV104	*ori*$V_{R6K\gamma}$ *ori*T_{RP4} *ori*V_{pES213} Kn^r *lacZ*α	17
pVSV107	*ori*$V_{R6K\gamma}$ *ori*T_{RP4} *ori*V_{pES213} Tp^r *lacZ*α	17

Continued on following page

TABLE 1—*Continued*

Strain, plasmid, or oligonucleotide	Relevant characteristics[a,b]	Source or reference
Oligonucleotides		
dma30	5′ GCCAGATCTGTCATTGGTTGGTGGACAGGCTAT 3′	This study
dma31	5′ CGGAGATCTCCCAGCCGATCAGTTTAGAGTA 3′	This study
dma52	5′ CTTCATGGCTCAAGGTGGTGGTTT 3′	This study
dma53	5′ GGCCTCCTAGATTAGGAGGCTTTG 3′	This study
dma54	5′ GGTTGTGGCAATGGAGTACTCAGTG 3′	This study
dma55	5′ TTCTGGGTTCCAATCGACACTTGG 3′	This study
dma56	5′ CCGCCCGGGCATGAAACGCTCCTTGTTATTTGTTC 3′	This study
dma57	5′ GCCCCCGGGTAAGTTCTTATACGTAACAACTGTGCTAC 3′	This study
dma58	5′ GGCAGATCTGGGCTGAAGCTGGGAAACTCAGTGATGATT 3′	This study
dma59	5′ CGGAGATCTTGCACGAATAGCAACACGAATTCGGCG 3′	This study
dma60	5′ CGGAGATCTCGTCAGCCTGAAAAGTTTACCGTGG 3′	This study
dma61	5′ CGGAGATCTCCGCACTCTTGGCTTGATTCTCTTT 3′	This study
dma62	5′ GGCAGATCTCGAATTGGTGAAGAGTATGGCGTTCAAC 3′	This study
dma63	5′ CGGAGATCTCCTAGCTCTTGCCATTGTGCTAACG 3′	This study
dma76	5′ GGCAGATCTCCTTAGAATCAACGGTAAGTACGCTAGAGTC 3′	This study
dma77	5′ CCGAGATCTGCTCAACTTGTTGTTGTGCTTGCTG 3′	This study
dma78	5′ GCCGGATCCGCAACAACCGCAGCCTTAGATTACATG 3′	This study
dma79	5′ GCCGGATCCGCAATGGCAAGATCTAACTGCTGCTT 3′	This study
dma95	5′ GCGTCTTTCAATCATTAGGCTACT 3′	This study
dma96	5′ CCGCGAAACCTGTTCGA 3′	This study
dma97	5′ GATTCATCAAGTACAGGTTCTTGGG 3′	This study
dma98	5′ CGGCCCGGGGGATCCTCAATACTTTAAATTCAGCTCTTTCTCGG 3′	This study
dma99	5′ CGGCCCGGGCATTGATTTCTTTAACACCTAAACTTTCCAA 3′	This study
dma100	5′ GCCCCCGGGTGATAAGTTTAAATTCTAATAGCAATTGGTATTAAGC 3′	This study
dma102	5′ GGCAAGAATATGACCAGCGTCGTTTTG 3′	This study
dma105	5′ CGGCCCGGGCATATAATTAATTCTCTTCTCTTGCTGCTTTATCT 3′	This study
dma106	5′ CGCCCCGGGTAACAGAGCAGGGTTCAGATCGCTTC 3′	This study
dma115	5′ TGGCTTTTTTCTGTGGTCTAAAAAA 3′	This study

[a] Abbreviations: Kn^r, kanamycin resistance; Str^r, streptomycin resistance; Tp^r, trimethoprim resistance.
[b] Underlined sequences indicate restriction enzyme recognition sites added to primers (BglII, A/GATCT; BamHI, G/GATCC; or SmaI, CCC/GGG).

Luminescence and motility assays. Motility and luminescence were assessed as described previously (1). Luminescence of cells cultured in SWTO (4) at 24°C was determined using a TD 20/20 luminometer (Turner Designs, Sunnyvale, CA). For motility assays, cultures were grown to mid-log phase (OD_{595} of 0.5) at 24°C, 5 μl of the culture was spotted onto a quadrant of an SWT soft (0.25%) agar plate, and diameter measurements of the movement away from the point of inoculation were taken every hour. For each spot, a slope estimate was obtained from a simple linear regression of diameter versus time to quantify the velocity of spread, defined as the motility rate.

Squid colonization assays. For infection with individual *V. fischeri* strains, *E. scolopes* juveniles were inoculated within 4 h of hatching as previously described (58). *E. scolopes* squid were maintained in Instant Ocean (Aquarium Systems, Mentor, OH) mixed to ~36 ppt, and cultures for inoculation were grown as previously described (17). Hatchlings were exposed to inocula for up to 14 h before being rinsed in *V. fischeri*-free Instant Ocean. To study infection kinetics, hatchlings were placed in 5 ml of inoculant in 20-ml glass vials and luminescence was monitored using an LS6500 scintillation counter (Beckman-Coulter, Fullerton, CA). To determine whether a mutant had a competitive disadvantage in the symbiosis relative to the wild type, animals were exposed to a ~1:1 mix of the wild-type and mutant strains for 14 h and then moved to *V. fischeri*-free Instant Ocean. Individual squid were homogenized and plated after 48 or 96 h, and 50 colonies were patched onto LBS-Em to determine the ratio of mutant to wild type. The relative competitive index was determined by dividing the mutant-to-wild-type ratio in each individual squid by the ratio in the inoculum. Log-transformed data were used to calculate the average relative competitive index and to determine statistical significance.

Assessment of how effectively juvenile squid colonized with one strain could be secondarily infected with another strain was performed as previously described (32, 73). Newly hatched animals were infected with the wild type or DMA388 as described above. At 72 h postinfection, approximately 2.5×10^4 CFU/ml of the secondary inoculant AKD200 (mini-Tn*7* Cm^r) was added for 14 h. At 120 h after the initial inoculation began, animals were homogenized and plated on LBS to determine total CFU and on LBS-Cm to estimate the proportion of symbionts from the secondary infection. Mini-Tn*7* Cm^r inserts at a single intergenic *att* site in *V. fischeri*, and this does not affect colonization competitiveness (39), making AKD200 an appropriate marked strain for this purpose.

Squid morphogenesis assays. Animals were infected with strains as described above. At the specified times after inoculation, infected and aposymbiotic animals were stained with both Cell Tracker orange and Tubulin Tracker green (Invitrogen, Carlsbad, CA) for approximately 1 h. After staining, animals were anesthetized by adding an equal volume of 0.37 M $MgCl_2$ and dissected to expose the light organ on the ventral side. Regression of the ciliated epithelial appendages was determined by epifluorescence microscopy with a Nikon (Melville, NY) Eclipse E600 microscope using a 51004 V2 fluorescein isothiocyanate-tetramethyl rhodamine isocyanate dual-label filter set (Chroma Technology Corp., Rockingham, VT) and/or a Nikon 96157 tetramethyl rhodamine isocyanate filter set. The latter filter set was used in conjunction with a Nikon Coolpix 5000 camera to obtain the epifluorescence images shown of animals stained with Cell Tracker. Regression stage (stages 0 to 4) was scored blindly, as set forth by Doino and McFall-Ngai (15). The *E. scolopes* light organ is bilobed, and each of the two lobes was scored separately, although we never observed an animal with lobes at different stages of regression. Images taken by scanning electron microscopy (SEM) are provided to help illustrate the appearance of regression stages, but animals were not scored for regression by SEM in this study.

RESULTS

Bioinformatic analysis of PG synthesis and recycling in *V. fischeri*. Before the 921-Da PG monomer known as TCT (13, 57) or PGCT (56, 62) can be released from gram-negative bacteria, it must first be generated intracellularly, and this occurs even in bacteria such as *E. coli* that do not shed PG monomers. Based on our understanding of *E. coli*, this PG monomer apparently is not generated during de novo PG synthesis but rather is produced during PG remodeling and consumed by recycling pathways (55). To examine whether de novo PG synthesis or PG recycling might be substantively different in *V. fischeri*, we examined its genome and found homologs of the *E. coli* PG synthesis and recycling pathways (see Table S1 in the supplemental material). Only minor deviations from the *E. coli* PG processing systems were evident. *V. fischeri* possesses only one homolog (AmiB) of the four amidases that may process PG monomer in the periplasm of *E. coli* (24, 68),

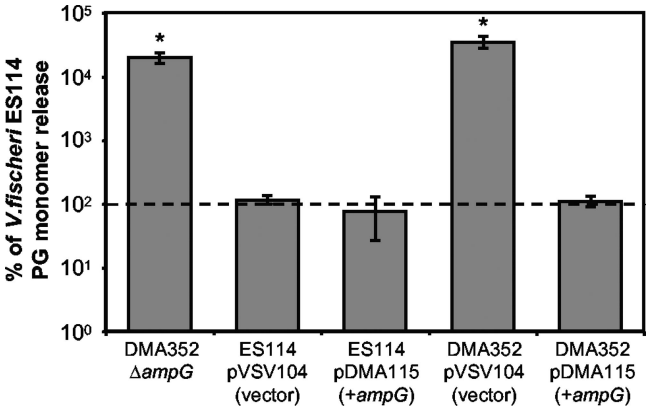

FIG. 1. Mutation in *V. fischeri ampG* increases net PG monomer release in log-phase cultures. PG monomer was measured in culture supernatants of ES114 (wild type) and DMA352 (Δ*ampG*) along with both strains containing plasmids pVSV104 (control vector) and pDMA115 (*ampG* in pVSV104). To account for experiment-to-experiment variations, within each experiment each strain's calculated PG monomer release was expressed as a percentage of ES114 PG monomer release. Values shown are the averages of three different experiments. The dotted line represents ES114 PG monomer release, defined as 100%, which averaged 20.4 nM per OD_{595}. Error bars are standard errors. Asterisks indicate significant differences ($P < 0.05$) from ES114 as determined by Student's *t* test.

but it seems reasonable that one such amidase might be sufficient. *V. fischeri* also lacks a clear homolog of LdcA, an L,D-carboxypeptidase found in the *E. coli* PG monomer recycling pathway (67); however, it does appear to encode distinct peptidases not found in *E. coli*, including a putative PG-targeting peptidase (encoded by ORF VF2017). Moreover, all of the functions downstream of LdcA in the recycling pathway appear intact. Based on these results, we speculated that *V. fischeri*'s net release of PG monomer might parallel either the poor *ampG* expression of *B. pertussis* or the high activity of lytic transglycosylases of *N. gonorrhoeae*, and we investigated these possibilities further.

Analysis of AmpG in *V. fischeri*. The single AmpG homolog found in BLAST searches of the *V. fischeri* genome is encoded by ORF VF0720, which shares 26% identity and 49% similarity with *E. coli* AmpG. The *V. fischeri* AmpG amino acid sequence is shorter than that of *E. coli* at the C terminus by 73 amino acids; however, *N. gonorrhoeae* AmpG is similarly shorter than *E. coli* AmpG by 77 amino acids, yet it has demonstrated functionality (18).

Mutation of *ampG* increases the net release of PG monomers. To test the functionality of *V. fischeri* AmpG in PG monomer recycling, we used an HPLC-based method for PG monomer detection (12, 31) to analyze the amount of PG monomer accumulated extracellularly during log-phase growth of DMA350 (*ampG*::pDMA48) relative to that of the wild type. We saw an increase in net PG monomer release from DMA350 (*ampG*::pDMA48) of approximately 39-fold (data not shown). Next, we generated an in-frame deletion mutant of *ampG* and found that DMA352 (Δ*ampG*) had more than a 100-fold increase in net PG monomer release (Fig. 1). This phenotype could be complemented by the introduction of *ampG* on a stable plasmid (pDMA115), decreasing the extracellular levels of PG monomer accumulation back to wild-type levels (Fig. 1). We occasionally saw a decrease in the amount of net PG monomer release when *ampG* was added in multicopy in *trans* to ES114; however, this result was not consistent from experiment to experiment, and this apparent slight effect is not statistically significant ($P > 0.05$; Fig. 1). These data suggest that *V. fischeri* AmpG is functional, and unlike the situation in *B. pertussis*, lack of AmpG is probably not responsible for the extracellular accumulation of PG monomers in cultures of *V. fischeri*.

Analysis of lytic transglycosylases in *V. fischeri*. In *N. gonorrhoeae* the activity of lytic transglycosylases is responsible for the large amounts of PG monomer accumulated in culture supernatants. Therefore, we examined whether *V. fischeri* had homologs to the *N. gonorrhoeae* lytic transglycosylases, LtgA and LtgD, which are important for release of PG monomers during log-phase growth in *N. gonorrhoeae* (9, 10). Two homologs to the *N. gonorrhoeae* LtgA sequence were found in *V. fischeri*, and these are encoded by VF0558 and VF1329 (see Table S1 in the supplemental material). VF0558, now termed *ltgA*, is well conserved in sequence and genetic context within the family *Vibrionaceae*, and the predicted amino acid sequence for *V. fischeri* LtgA has 24% identity and 43% similarity to that for *N. gonorrhoeae* LtgA. VF0558 and *N. gonorrhoeae* LtgA were best matches in reciprocal genome searches, leading to the designation of VF0558 as *ltgA*. The other LtgA-like protein, encoded by VF1329, is now designated *ltgY* to distinguish it from *ltgA* (VF0558) while avoiding the names of genes such as *ltgB* or *ltgC* that encode more-dissimilar proteins in *N. gonorrhoeae*. The *ltgY* gene is related to *ltgA* but appeared absent from the other members of the *Vibrionaceae* family that we examined. The predicted amino acid sequence of LtgY shares 34% identity and 55% similarity with that of *V. fischeri* LtgA and 24% identity and 42% similarity with that of *N. gonorrhoeae* LtgA. Only one homolog to *N. gonorrhoeae* LtgD was found in *V. fischeri*, and this is encoded by VF1702. A reciprocal search found that in the *N. gonorrhoeae* FA1090 genome LtgD is likewise the protein most similar to that encoded by VF1702. This *V. fischeri* gene, now termed *ltgD*, has a conserved upstream genetic context within the *Vibrionaceae* family, although the downstream genetic context is different. The predicted amino acid sequence of *V. fischeri* LtgD had 30% identity and 48% similarity to the *N. gonorrhoeae* LtgD sequence.

We also searched the ES114 genome for other genes potentially encoding lytic transglycosylases. Two ORFs, VF1939 and VF1247, were found to encode LysM domains that are important in general PG binding and have the potential to be PG hydrolases (6). These ORFs were named *ltgE* and *lysM*, respectively. Based on genome comparisons, VF1247 (*ltgE*) encodes a reciprocal best match to both the membrane-bound lytic murein transglycosylase MltD in *E. coli* (see Table S1 in the supplemental material) and LtgE in *N. gonorrhoeae*. We have designated VF1247 as *ltgE* to be consistent with the nomenclature in *N. gonorrhoeae* (10).

Mutations in lytic transglycosylase genes result in reduced net release of PG monomers. To determine if any of these putative lytic transglycosylases were responsible for the release of PG monomers by *V. fischeri*, we generated plasmid integration mutants yielding DMA360 (*ltgA*::pDMA89), DMA361 (*ltgY*::pDMA90), DMA362 (*ltgD*::pDMA91), DMA380 (*ltgE*::

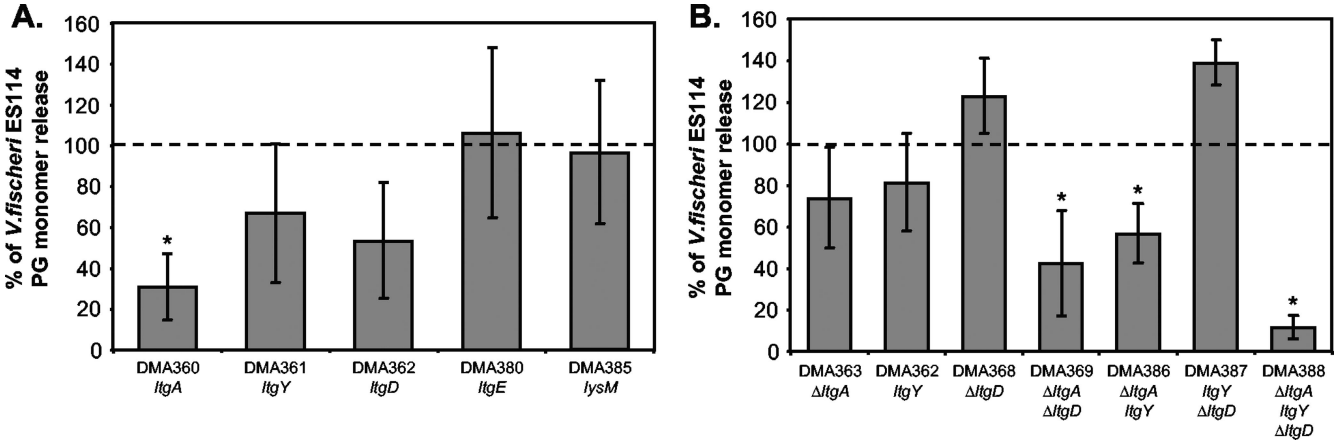

FIG. 2. Mutations in *V. fischeri* lytic transglycosylases result in a decrease in net PG monomer release in log-phase cultures. Values are the averages of three different experiments ± standard errors. The dotted line represents ES114 PG monomer release, defined as 100%. Asterisks in both panels indicate significant differences ($P < 0.05$) from ES114 as determined by Student's *t* test. (A) Plasmid-insertion mutants with disruptions in *ltgA*, *ltgY*, *ltgD*, *ltgE*, and *lysM*. The wild type averaged 28 nM per OD_{595}. (B) Comparison of mutants with combinations of in-frame deletion mutations Δ*ltgA* and Δ*ltgD* and a plasmid-insertion mutation in *ltgY*. The wild type for this set of experiments averaged 14 nM per OD_{595}.

pDMA109), and DMA385 (*lysM*::pDMA108). We then assayed the effects of the mutations on net PG monomer release as described above. DMA360 (*ltgA*::pDMA89) had threefold-less net PG monomer release than did the wild type (Fig. 2A). Similarly, DMA361 (*ltgY*::pDMA90) and DMA362 (*ltgD*::pDMA91) each appeared to accumulate fewer PG monomers in culture supernatants than did the wild type, but these differences were not significant ($P > 0.05$). Finally, both DMA380 (*ltgE*::pDMA109) and DMA385 (*lysM*::pDMA108) appeared unaffected in net PG monomer release (Fig. 2A).

In *N. gonorrhoeae* multiple mutations in the lytic transglycosylase genes are necessary to drastically reduce the accumulation of PG monomer in cultures. To determine whether this might be the case in *V. fischeri*, we constructed in-frame deletions of *ltgA* and *ltgD*, resulting in DMA363 (Δ*ltgA*) and DMA368 (Δ*ltgD*), respectively. These alleles were combined with the *ltgY*::pDMA90 allele construct both in pairwise combinations and to generate a triple mutant. The Δ*ltgA* allele combined with other mutations resulted in significantly less extracellular accumulation of PG monomer. This was true for DMA369 (Δ*ltgA* Δ*ltgD*), DMA386 (Δ*ltgA ltgY*::pDMA90), and DMA388 (Δ*ltgA* Δ*ltgD ltgY*::pDMA90), the last of which has very low (2 ± 1 nM per OD_{595}) levels of PG monomer in culture supernatants (Fig. 2B).

It is not clear why the *ltgA*::pDMA89 mutation appears to have a greater effect on PG monomer release (Fig. 2A) than does the Δ*ltgA* allele (Fig. 2B). We cannot rule out the possibility that allelic differences affect PG monomer release—for example, if a truncated LtgA in the *ltgA*::pDMA89 mutant interfered with other lytic transglycosylases; however, this apparent difference between mutants may simply reflect variability in this assay, as the *ltgA*::pDMA89 and Δ*ltgA* mutants were not examined together. In this regard, it should be noted that the amount of PG monomer measured in supernatants from the wild type was smaller for the experiment in Fig. 2B than it was for the experiment in Fig. 2A (see figure legend), and the unusually low value for the wild type in Fig. 2B alone could explain why PG monomer released by the mutants expressed as a percentage of the wild-type value would appear higher in this data set.

Growth, motility, and luminescence of *ampG* and lytic transglycosylase mutants. Mutations affecting recycling and remodeling of PG could affect cell division, growth, motility, and even metabolism. However, all mutants had wild-type-like growth, cell morphology, and bioluminescence (data not shown), indicating that these are not generally attenuated strains. Mutants also had at least 80% to 99% motility relative to that of the wild type (data not shown), and a previous study found that these swimming rates are sufficient to confer full symbiotic competence (1).

Symbiotic competence of DMA352 (Δ*ampG*) and DMA388 (Δ*ltgA* Δ*ltgD ltgY*::pDMA90). One of our goals was to examine the effect of altered extracellular PG monomer accumulation on symbiotic colonization. We therefore examined the symbiotic competence of the mutants with the greatest deviations in net PG monomer release; DMA352 (Δ*ampG*) and DMA388 (Δ*ltgA* Δ*ltgD ltgY*::pDMA90). In single-strain infections of squid, neither DMA352 nor DMA388 showed a difference from the wild type (data not shown). Competition experiments have been used previously as a measure of relative symbiotic proficiency, revealing colonization defects not apparent in single-strain inoculations (4, 29, 32, 34, 35, 46, 53, 64, 70, 71, 74, 75). However, there was no apparent competitive defect 48 h or 96 h postinoculation when either DMA352 (Δ*ampG*) or DMA388 (Δ*ltgA* Δ*ltgD ltgY*::pDMA90) was coinoculated along with the wild type (data not shown).

Mutant effects on host light-organ morphogenesis. Because PG monomers act as a morphogen triggering regression of the ciliated appendages on the light organ (31), we investigated whether mutations affecting the net amount of PG monomer released would alter this morphogenesis. Animals inoculated with DMA352 (Δ*ampG*) and examined at 24-h intervals up to 120 h showed ciliated appendage regression similar to that in animals infected with the wild type. Thus, the ~100-fold increase in net PG monomer release by the *ampG* mutant in

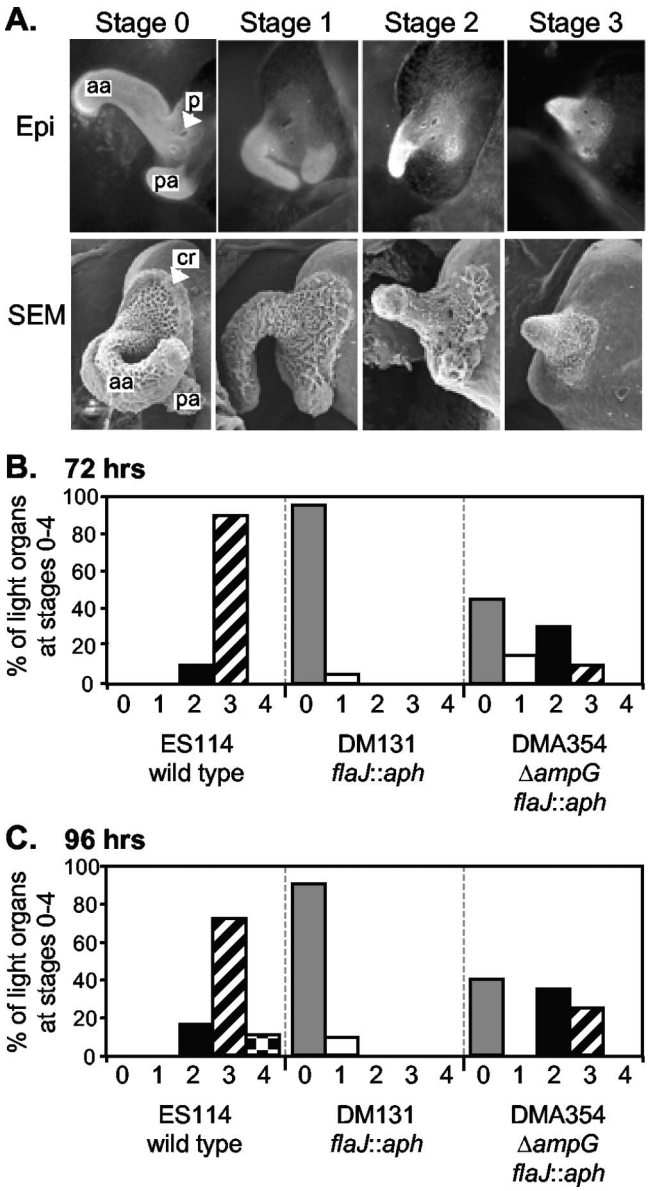

FIG. 3. A nonmotile *ampG* mutant triggers regression of the ciliated appendages of the light organ. (A) Light-organ ciliated appendages observed by epifluorescence microscopy (Epi) and SEM to illustrate regression stages. Each image is approximately 100-fold enlarged and shows one lobe of a roughly symmetrical bilobed organ. Labels: aa, anterior appendage; pa, posterior appendage; p, one of three closely grouped pores (indicated only in epifluorescence image); cr, ciliated ridge (indicated only in SEM image). Epifluorescence images highlight epithelial cells in the appendages stained with Cell Tracker orange, and SEM images show the fuzzy appearance of the cilia extending from such epithelial cells. In stage 1 regression, fields of ciliated cells thin out, notably in the ciliated ridge and anterior appendage, but both appendages are still present. In stage 2, the posterior appendage is only a nub and the anterior appendage has shortened. In stage 3, the anterior appendage is a nub and the posterior appendage is absent. Stage 4 is not pictured and represents the complete loss of ciliated appendages, as described by Doino and McFall-Ngai (15). (B and C) Freshly hatched juvenile animals were inoculated with ~2,500 CFU/ml of either ES114 (wild type), DM131 (*flaJ*::*aph*), or DMA354 (Δ*ampG flaJ*::*aph*), each of which was labeled with the *gfp*-expressing plasmid pVSV102 to confirm that the nonmotile *flaJ* mutants did not infect the interior light-organ crypts. Animals were stained at 72 h (B) or 96 h (C) postinoculation and scored blindly for regression stage as illustrated in panel A. The data presented are combined from three experiments scored at 72 h and three scored at 96 h, with similar results among each set of three experiments. Twenty to 21 animals inoculated with each strain were scored at 72 h, and 18 to 21 animals inoculated with each strain were scored at 96 h.

culture did not appear to correlate with more rapid regression of the ciliated appendages.

We next examined whether the *ampG* mutation could trigger morphogenesis in a strain that could not colonize the light-organ crypts. Nonmotile *V. fischeri* strains do not enter the light-organ crypts and do not induce regression (15), although they are able to induce mucus production from the ciliated fields and can form aggregates outside the pores of the light organ (53). We therefore tested whether a nonmotile strain generating large amounts of extracellular PG monomer might be able to induce regression without colonizing the light-organ crypt, by constructing a *flaJ ampG* double mutant. We then compared morphogenesis in animals inoculated with the wild type, DM131 (*flaJ*::*aph*), or DMA354 (Δ*ampG flaJ*::*aph*). To ensure that the nonmotile *flaJ* mutants did not infect the light-organ crypts, each of the three strains used was labeled with the stable *gfp*-expressing plasmid pVSV102 (17), and epifluorescence microscopy confirmed that only wild-type cells could be visualized colonizing the crypts.

At 72 and 96 h postinoculation, wild-type-infected animals all displayed regression of the ciliated epithelial appendages (Fig. 3). In contrast, animals infected with DM131 (*flaJ*::*aph*) displayed essentially no regression (a few animals were scored at stage 1 regression), consistent with previous reports comparing the wild type to nonmotile mutants (21, 45). However, more than half of the animals inoculated with DMA354 (Δ*ampG flaJ*::*aph*) showed regression, with some animals progressing as far as stage 3 (Fig. 3), even though the *flaJ* mutation blocked invasion of the light-organ crypts. We considered the possibility that PG monomer already present in the inoculum might be inducing regression, as Koropatnick et al. observed with as little as 10 nM purified PG monomer (31); however, assuming that net PG monomer release was similar under the growth conditions used to prepare inocula to the net PG monomer release in minimal media, then carryover of PG monomer from the inoculum should have resulted in animals being exposed to only ~10 pM PG monomer in these experiments. Moreover, similar results were obtained when DMA354 (Δ*ampG flaJ*::*aph*) cells were washed in Instant Ocean before hatchlings were exposed to them. This result suggests that the regression induced by DMA354 (Δ*ampG flaJ*::*aph*) is due to bacteria aggregating and shedding high levels of PG monomer in situ, on the light organ.

Our next goal was to see if the small amount of net PG monomer release by the lytic transglycosylase mutant DMA388 (Δ*ltgA* Δ*ltgD ltgY*::pDMA90) would reduce the stimulation of morphogenesis. It did appear that there was less regression of the ciliated appendages in animals infected with DMA388 (Δ*ltgA* Δ*ltgD ltgY*::pDMA90) than in animals infected with the wild type; however, using the semiquantitative scoring of regression stages 0 to 4 defined previously (15), we did not see a consistent and statistically significant difference in these treatments (data not shown). We also observed what appeared to be more dense and active fields of cilia on the appendages of DMA388-

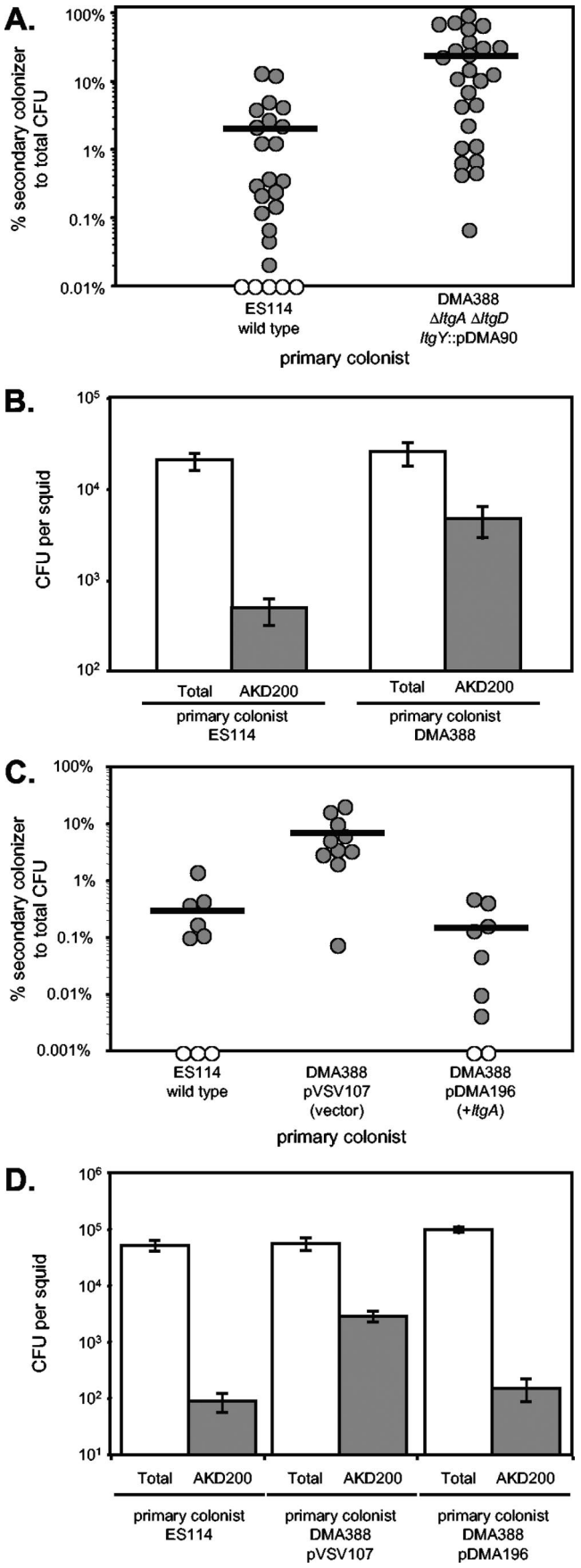

infected animals, but again we were unable to quantify and adequately test this supposition. We therefore sought another way to measure the status of the ciliated appendages. We surmised that, if some animals retained their infection-promoting ciliated appendages longer, these animals might be more susceptible to a secondary infection with another bacterial strain presented well after initial infection. To address this experimentally, animals were inoculated following hatching with either the wild-type strain or DMA388 (Δ*ltgA* Δ*ltgD ltgY*::pDMA90), and at 72 h after inoculation with the primary strain, animals were exposed to a secondary inoculant strain, AKD200 (mini-Tn*7* Cm^r). At 120 h post-primary inoculation (i.e., 48 h post-secondary inoculation), animals were homogenized and plated on LBS to assess total colonization and plated on LBS-Cm to enumerate bacteria from the secondary infection. DMA388-infected animals had 10-fold-more bacteria from the secondary AKD200 infection than did wild-type-infected animals (Fig. 4A and B) and were complemented by the addition of *ltgA* on a stable multicopy plasmid (Fig. 4C and D). Thus, DMA388-infected animals are more prone to secondary infection, consistent with our perception that the infection-promoting ciliated appendages were more intact in these animals.

DISCUSSION

A specific 921-Da component of gram-negative PG referred to here as PG monomer (and elsewhere as TCT or PGCT) is usually recycled by bacterial cells, but in instances where PG monomer is released in significant amounts, it elicits dramatic effects on host epithelial tissues. When released by the pathogen *B. pertussis* or *N. gonorrhoeae*, PG monomer causes severe cytopathology in ciliated human epithelial cells (12, 42). PG monomer is also released by the mutualistic symbiont *V. fischeri*, and in its natural host squid, purified PG monomer triggers regression of ciliated epithelial appendages of the symbiotic

FIG. 4. Animals infected with DMA388 (Δ*ltgA* Δ*ltgD ltgY*::pDMA90) are more susceptible to a secondary infection. Hatchlings were inoculated with either ES114, DMA388 (Δ*ltgA* Δ*ltgD ltgY*::pDMA90), DMA388 pVSV107, or DMA388 pDMA196 (*ltgA*). After 72 h, animals were inoculated with the secondary strain AKD200 (mini-Tn*7* Cm^r). At 120 h, animals were homogenized and plated to determine both total CFU and Cm^r CFU corresponding to the secondary colonizers. Values in panels A and B are the combined averages of six independent experiments, all of which yielded similar results (total $n = 25$ for ES114 and $n = 26$ for DMA388). Values in panels C and D are the combined averages of two independent experiments, which yielded similar results (total $n = 9$ for ES114, $n = 10$ for DMA388 pVSV107, and $n = 10$ for DMA388 pDMA196). (A and C) Percentages of total infection comprised by the secondary colonist, AKD200. Each circle represents a single squid. Open circles represent animals below the limit of detection for Cm^r cells. Horizontal lines show the averages of all animals within each treatment (panel A, 2% in ES114-infected animals, and 24% in DMA388-infected animals; panel C, 0.3% in ES114-infected animals, 7.4% in DMA388 pVSV107-infected animals, and 0.2% in DMA388 pDMA196-infected animals). (B and D) Averages of both total CFU (open bars) and CFU from secondary infection by AKD200 (shaded bars). Error bars are standard errors. Student *t* tests indicated that secondary infection by AKD200 in DMA388-infected animals was significantly greater ($P < 0.01$) than that in ES114-infected animals in panel B and that secondary infection by AKD200 in DMA388 pVSV107-infected animals was significantly greater ($P < 0.05$) than that in ES114- or DMA388 pDMA196-infected animals in panel D.

light organ, reminiscent of the normal developmental program induced in this symbiosis (31). In this study we generated mutants of *V. fischeri* that displayed either increased or decreased extracellular accumulation of PG monomer, providing insight into the basis for PG monomer shedding in this bacterium and the role of PG monomers in this model mutualistic infection.

We first examined the genetic determinants of PG monomer release in *V. fischeri*. In contrast to *B. pertussis*, where extracellular PG monomer accumulation is thought to be a result of poor *ampG* expression (36), *V. fischeri* AmpG functioned well in reducing net PG monomer release, as illustrated by the 100-fold increase in PG accumulated in the medium of an *ampG* mutant and by the observation that overexpressing *ampG* from *V. fischeri* or *E. coli* did little to lessen net PG monomer release (Fig. 1 and data not shown, respectively). *V. fischeri* apparently also has a complete recycling pathway (see Table S1 in the supplemental material), suggesting that *V. fischeri* recycles PG monomers as other gram-negative bacteria do. Apparently, the basis for *V. fischeri*'s extracellular accumulation of PG monomers is more similar to that of *N. gonorrhoeae*, where the deletion of two lytic transglycosylases results in the reduced net release of PG monomers (9, 10). In *V. fischeri*, mutation of multiple lytic transglycosylases similar to those in *N. gonorrhoeae* also reduced net PG monomer release (Fig. 2B).

The generation of mutants with more or less extracellular accumulation of PG monomer than that of the wild type enabled us to evaluate the importance of this molecule in vivo during symbiotic infection. When squid were inoculated with DMA352 (Δ*ampG*), which accumulates 100-fold-more PG monomers in culture supernatants than does the wild type (Fig. 1), we did not see a faster progression of light-organ morphogenesis (data not shown). This is consistent with the idea that PG monomer elicits effects on the host as a triggering signal molecule and that the wild type sheds sufficient PG monomer to trigger these effects. Interestingly, we did show that a *flaJ ampG* double mutant was able to induce regression of the ciliated light-organ appendages (Fig. 3B and C), unlike the *flaJ* mutant and other nonmotile mutants. Nonmotile mutants will aggregate around the light-organ pores, but they are unable to colonize the light-organ crypt spaces (21, 53). The inability of these mutants to stimulate morphogenesis has suggested a requirement for crypt infection in signal transduction (15), although it was subsequently shown that purified PG monomer added to seawater can stimulate morphogenesis (31). The *flaJ ampG* double mutant demonstrates that crypt infection is not necessary for PG-mediated signaling, and this strain should be a useful tool for separating PG monomer-mediated signaling from signaling that truly requires infection of the crypts. In the future, it also will be interesting to compare the effects of this mutant to the effects of purified PG monomer, to explore possible PG-independent signaling factors that may be perceived by the host from symbionts still on the light-organ surface.

We also investigated DMA388 (Δ*ltgA* Δ*ltgD ltgY*::pDMA90), which accumulates only low levels of PG monomer in culture (Fig. 2). We hypothesized that this strain would have reduced regression of the ciliated light-organ appendages; however, it still induced regression of the ciliated appendages. A reason for this could be that another lytic transglycosylase is induced only in the symbiosis, supplying a mechanism for PG monomer release that is not evident in culture. By creating *gfp*-based transcriptional reporters of each of the lytic transglycosylase genes listed in Table S1 in the supplemental material, we may be able to determine if any of the genes are transcriptionally activated when *V. fischeri* is within the squid. It is also possible that a small amount of PG monomer released by this strain is sufficient to stimulate morphogenesis or that other PG fragments besides the 921-Da fragment could have an effect on regression. A reduced version of the PG monomer is also released by *V. fischeri* (data not shown), and this or other PG fragments might have important morphogenic activity.

Despite the morphogenesis induced by DMA388 (Δ*ltgA* Δ*ltgD ltgY*::pDMA90), we did perceive a subtle attenuation of this strain's ability to stimulate regression of the host's light-organ ciliated appendages. A more dramatic or at least more easily quantifiable effect was evident in the greater susceptibility of DMA388-infected animals to a secondary *V. fischeri* colonist after regression of the infection-promoting ciliated appendages had begun (Fig. 4). This suggests that even an apparently small difference in the regression of the ciliated appendages may have large functional significance with regard to preventing or allowing further infection by environmental bacteria. In the future it will be interesting to examine the effects of DMA388 on specific infection-promoting characteristics of the ciliated appendages, such as water movement and mucus secretion (41, 50–53).

The dramatic regression of the infection-promoting ciliated appendages on the *E. scolopes* light organ following successful infection with *V. fischeri* symbionts can be easily rationalized as an advantage for the host. This morphogenesis effectively deters further infection, and if these infection-promoting structures carry any risk of promoting detrimental pathogenic infections, then the risks associated with these structures may outweigh the advantages once mutualistic symbionts are obtained. Our results illustrate how *V. fischeri* may also have an evolutionary impetus for shedding PG monomers. By stimulating morphogenesis, PG monomers help *V. fischeri* to essentially close the door behind them after initial infection. A secondary infection with another strain would create competition within the light organ, potentially causing the initial colonizer to lose some of the fitness advantage of colonizing the light organ. Initiating the regression of the ciliated epithelial appendages therefore enhances the initial colonizer's ability to maintain dominance in the light organ. Further use of secondary-infection challenge assays should be valuable in the future, because mutants that lack the ability to prevent secondary infections could reveal genes important for stimulating regression of the ciliated appendages that may not be found using other screens.

ACKNOWLEDGMENTS

We thank Joshua Troll, Melissa Altura, and Amy Schaeffer for helpful discussions; Joseph Dillard for sharing data on *ltgD* before publication; William Swinehart for technical assistance; and Debbie Millikan, Edward Ruby, and Anne Dunn for providing strains.

This work was supported by the National Institutes of Health under grant A150661 to M.J.M.-N. and by the National Science Foundation under grant Career MCB-0347317 to E.V.S.

REFERENCES

1. **Adin, D. M., N. J. Phillips, B. W. Gibson, M. A. Apicella, E. G. Ruby, M. J. McFall-Ngai, D. B. Hall, and E. V. Stabb.** 2008. Characterization of *htrB* and *msbB* mutants of the light organ symbiont *Vibrio fischeri*. Appl. Environ. Microbiol. **74:**633–644.
2. **Altschul, S. F., W. Gish, W. Miller, E. W. Myers, and D. J. Lipman.** 1990. Basic local alignment search tool. J. Mol. Biol. **215:**403–410.
3. **Boettcher, K. J., and E. G. Ruby.** 1990. Depressed light emission by symbiotic *Vibrio fischeri* of the sepiolid squid *Euprymna scolopes*. J. Bacteriol. **172:** 3701–3706.
4. **Bose, J. L., U. Kim, W. Bartkowski, R. P. Gunsalus, A. M. Overley, N. L. Lyell, K. L. Visick, and E. V. Stabb.** 2007. Bioluminescence in *Vibrio fischeri* is controlled by the redox-responsive regulator ArcA. Mol. Microbiol. **65:** 538–553.
5. **Bose, J. L., C. S. Rosenberg, and E. V. Stabb.** 2008. Enhancement of symbiotic colonization and conditional attenuation of growth in culture. Arch. Microbiol. **190:**169–183.
6. **Buist, G., A. Steen, J. Kok, and O. P. Kuipers.** 2008. LysM, a widely distributed protein motif for binding to (peptido)glycans. Mol. Microbiol. **68:**838–847.
7. **Campanella, J. J., L. Bitincka, and J. Smalley.** 2003. MatGAT: an application that generates similarity/identity matrices using protein or DNA sequences. BMC Bioinformatics **4:**29.
8. **Chen, C. Y., K. M. Wu, Y. C. Chang, C. H. Chang, H. C. Tsai, T. L. Liao, Y. M. Liu, H. J. Chen, A. B. Shen, J. C. Li, T. L. Su, C. P. Shao, C. T. Lee, L. I. Hor, and S. F. Tsai.** 2003. Comparative genome analysis of *Vibrio vulnificus*, a marine pathogen. Genome Res. **13:**2577–2587.
9. **Cloud, K. A., and J. P. Dillard.** 2002. A lytic transglycosylase of *Neisseria gonorrhoeae* is involved in peptidoglycan-derived cytotoxin production. Infect. Immun. **70:**2752–2757.
10. **Cloud-Hansen, K. A., K. T. Hackett, D. L. Garcia, and J. P. Dillard.** 2008. *Neisseria gonorrhoeae* uses two lytic transglycosylases to produce cytotoxic peptidoglycan monomers. J. Bacteriol. **190:**5989–5994.
11. **Cloud-Hansen, K. A., S. B. Peterson, E. V. Stabb, W. E. Goldman, M. J. McFall-Ngai, and J. Handelsman.** 2006. Breaching the great wall: peptidoglycan and microbial interactions. Nat. Rev. Microbiol. **4:**710–716.
12. **Cookson, B. T., H.-L. Cho, L. A. Herwaldt, and W. E. Goldman.** 1989. Biological activities and chemical composition of purified tracheal cytotoxin of *Bordetella pertussis*. Infect. Immun. **57:**2223–2229.
13. **Cookson, B. T., A. N. Tyler, and W. E. Goldman.** 1989. Primary structure of the peptidoglycan-derived tracheal cytotoxin of *Bordetella pertussis*. Biochemistry **28:**1744–1749.
14. **Demchick, P., and A. L. Koch.** 1996. The permeability of the wall fabric of *Escherichia coli* and *Bacillus subtilis*. J. Bacteriol. **178:**768–773.
15. **Doino, J. A., and M. J. McFall-Ngai.** 1995. A transient exposure to symbiosis-competent bacteria induces light organ morphogenesis in the host squid. Biol. Bull. **189:**347–355.
16. **Dunn, A. K., M. O. Martin, and E. V. Stabb.** 2005. Characterization of pES213, a small mobilizable plasmid from *Vibrio fischeri*. Plasmid **54:**114–134.
17. **Dunn, A. K., D. S. Millikan, D. M. Adin, J. L. Bose, and E. V. Stabb.** 2006. New *rfp*- and pES213-derived tools for analyzing symbiotic *Vibrio fischeri* reveal patterns of infection and *lux* expression in situ. Appl. Environ. Microbiol. **72:**802–810.
18. **Garcia, D. L., and J. P. Dillard.** 2008. Mutations in *ampG* or *ampD* affect peptidoglycan fragment release from *Neisseria gonorrhoeae*. J. Bacteriol. **190:**3799–3807.
19. **Gittins, J. R., D. A. Phoenix, and J. M. Pratt.** 1994. Multiple mechanisms of membrane anchoring of *Escherichia coli* penicillin-binding proteins. FEMS Microbiol. Rev. **13:**1–12.
20. **Goodell, E. W.** 1985. Recycling of murein by *Escherichia coli*. J. Bacteriol. **163:**305–310.
21. **Graf, J., P. V. Dunlap, and E. G. Ruby.** 1994. Effect of transposon-induced motility mutations on colonization of the host light organ by *Vibrio fischeri*. J. Bacteriol. **176:**6986–6991.
22. **Hanahan, D.** 1983. Studies on transformation of *Escherichia coli* with plasmids. J. Mol. Biol. **166:**557–580.
23. **Heidelberg, J. F., J. A. Eisen, W. C. Nelson, R. A. Clayton, M. L. Gwinn, R. J. Dodson, D. H. Haft, E. K. Hickey, J. D. Peterson, L. Umayam, S. R. Gill, K. E. Nelson, T. D. Read, H. Tettelin, D. Richardson, M. D. Ermolaeva, J. Vamathevan, S. Bass, H. Qin, I. Dragoi, P. Sellers, L. McDonald, T. Utterback, R. D. Fleishmann, W. C. Nierman, O. White, S. L. Salzberg, H. O. Smith, R. R. Colwell, J. J. Mekalanos, J. C. Venter, and C. M. Fraser.** 2000. DNA sequence of both chromosomes of the cholera pathogen *Vibrio cholerae*. Nature **406:**477–483.
24. **Heidrich, C., M. F. Templin, A. Ursinus, M. Merdanovic, J. Berger, H. Schwarz, M. A. de Pedro, and J. V. Höltje.** 2001. Involvement of *N*-acetylmuramyl-L-alanine amidases in cell separation and antibiotic-induced autolysis of *Escherichia coli*. Mol. Microbiol. **41:**167–178.
25. **Heidrich, C., A. Ursinus, J. Berger, H. Schwarz, and J. V. Höltje.** 2002. Effects of multiple deletions of murein hydrolases on viability, septum cleavage, and sensitivity to large toxic molecules in *Escherichia coli*. J. Bacteriol. **184:**6093–6099.
26. **Henikoff, S., and J. G. Henikoff.** 1992. Amino acid substitution matrices from protein blocks. Proc. Natl. Acad. Sci. USA **89:**10915–10919.
27. **Herrero, M., V. de Lorenzo, and K. N. Timmis.** 1990. Transposon vectors containing non-antibiotic resistance selection markers for cloning and stable chromosomal insertion of foreign genes in gram-negative bacteria. J. Bacteriol. **172:**6557–6567.
28. **Höltje, J. V., D. Mirelman, N. Sharon, and U. Schwarz.** 1975. Novel type of murein transglycosylase in *Escherichia coli*. J. Bacteriol. **124:**1067–1076.
29. **Hussa, E. A., T. M. O'Shea, C. L. Darnell, E. G. Ruby, and K. L. Visick.** 2007. Two-component response regulators of *Vibrio fischeri*: identification, mutagenesis, and characterization. J. Bacteriol. **189:**5825–5838.
30. **Jacobs, C., L. J. Huang, E. Bartowsky, S. Normark, and J. T. Park.** 1994. Bacterial cell wall recycling provides cytosolic muropeptides as effectors for beta-lactamase induction. EMBO J. **13:**4684–4694.
31. **Koropatnick, T. A., J. T. Engle, M. A. Apicella, E. V. Stabb, W. E. Goldman, and M. J. McFall-Ngai.** 2004. Microbial factor-mediated development in a host-bacterial mutualism. Science **306:**1186–1188.
32. **Lee, K.-H., and E. G. Ruby.** 1994. Competition between *Vibrio fischeri* strains during initiation and maintenance of a light organ symbiosis. J. Bacteriol. **176:**1985–1991.
33. **Lindquist, S., K. Weston-Hafer, H. Schmidt, C. Pul, G. Korfmann, J. Erickson, C. Sanders, H. H. Martin, and S. Normark.** 1993. AmpG, a signal transducer in chromosomal beta-lactamase induction. Mol. Microbiol. **9:**703–715.
34. **Lupp, C., R. E. Hancock, and E. G. Ruby.** 2002. The *Vibrio fischeri sapABCDF* locus is required for normal growth, both in culture and in symbiosis. Arch. Microbiol. **179:**57–65.
35. **Lupp, C., M. Urbanowski, E. P. Greenberg, and E. G. Ruby.** 2003. The *Vibrio fischeri* quorum-sensing systems *ain* and *lux* sequentially induce luminescence gene expression and are important for persistence in the squid host. Mol. Microbiol. **50:**319–331.
36. **Lyon, R. S.** 2001. Tracheal cytotoxin production by the *Bordetellae.* Ph.D. thesis. Washington University, St. Louis, MO.
37. **Makino, K., K. Oshima, K. Kurokawa, K. Yokoyama, T. Uda, K. Tagomori, Y. Iijima, M. Najima, M. Nakano, A. Yamashita, Y. Kubota, S. Kimura, T. Yasunaga, T. Honda, H. Shinagawa, M. Hattori, and T. Iida.** 2003. Genome sequence of *Vibrio parahaemolyticus*: a pathogenic mechanism distinct from that of *Vibrio cholerae*. Lancet **361:**743–749.
38. **Martin, S. A., R. S. Rosenthal, and K. Biemann.** 1987. Fast atom bombardment mass spectrometry and tandem mass spectrometry of biologically active peptidoglycan monomers from *Neisseria gonorrhoeae*. J. Biol. Chem. **262:** 7514–7522.
39. **McCann, J., E. V. Stabb, D. S. Millikan, and E. G. Ruby.** 2003. Population dynamics of *Vibrio fischeri* during infection of *Euprymna scolopes*. Appl. Environ. Microbiol. **69:**5928–5934.
40. **McFall-Ngai, M. J.** 1994. Animal-bacterial interactions in the early life history of marine invertebrates: the *Euprymna scolopes*/*Vibrio fischeri* symbiosis. Am. Zool. **34:**554–561.
41. **McFall-Ngai, M. J., and E. G. Ruby.** 1991. Symbiont recognition and subsequent morphogenesis as early events in an animal-bacterial mutualism. Science **254:**1491–1494.
42. **Melly, M. A., Z. A. McGee, and R. S. Rosenthal.** 1984. Ability of monomeric peptidoglycan fragments from *Neisseria gonorrhoeae* to damage human fallopian-tube mucosa. J. Infect. Dis. **149:**378–386.
43. **Mielcarek, N., A. S. Debrie, D. Raze, J. Bertout, C. Rouanet, A. B. Younes, C. Creusy, J. Engle, W. E. Goldman, and C. Locht.** 2006. Live attenuated *B. pertussis* as a single-dose nasal vaccine against whooping cough. PLoS Pathog. **2:**e65.
44. **Miller, J. H.** 1992. A short course in bacterial genetics. Cold Spring Harbor Laboratory Press, Cold Spring Harbor, NY.
45. **Millikan, D. S., and E. G. Ruby.** 2003. FlrA, a σ^{54}-dependent transcriptional activator in *Vibrio fischeri*, is required for motility and symbiotic light-organ colonization. J. Bacteriol. **185:**3547–3557.
46. **Millikan, D. S., and E. G. Ruby.** 2004. *Vibrio fischeri* flagellin A is essential for normal motility and for symbiotic competence during initial squid light organ colonization. J. Bacteriol. **186:**4315–4325.
47. **Montgomery, M. K., and M. J. McFall-Ngai.** 1994. Bacterial symbionts induce host organ morphogenesis during early postembryonic development of the squid *Euprymna scolopes*. Development **120:**1719–1729.
48. **Montgomery, M. K., and M. J. McFall-Ngai.** 1993. Embryonic development of the light organ of the sepiolid squid *Euprymna scolopes* Berry. Biol. Bull. **184:**296–308.
49. **Nelson, D. E., A. S. Ghosh, A. L. Paulson, and K. D. Young.** 2002. Contribution of membrane-binding and enzymatic domains of penicillin binding protein 5 to maintenance of uniform cellular morphology of *Escherichia coli*. J. Bacteriol. **184:**3630–3639.
50. **Nyholm, S. V., B. Deplancke, H. R. Gaskins, M. A. Apicella, and M. J. McFall-Ngai.** 2002. Roles of *Vibrio fischeri* and nonsymbiotic bacteria in the dynamics of mucus secretion during symbiont colonization of the *Euprymna scolopes* light organ. Appl. Environ. Microbiol. **68:**5113–5122.

51. **Nyholm, S. V., and M. J. McFall-Ngai.** 2003. Dominance of *Vibrio fischeri* in secreted mucus outside the light organ of *Euprymna scolopes*: the first site of symbiont specificity. Appl. Environ. Microbiol. **69:**3932–3937.
52. **Nyholm, S. V., and M. J. McFall-Ngai.** 2004. The winnowing: establishing the squid-vibrio symbiosis. Nat. Rev. Microbiol. **2:**632–642.
53. **Nyholm, S. V., E. V. Stabb, E. G. Ruby, and M. J. McFall-Ngai.** 2000. Establishment of an animal-bacterial association: recruiting symbiotic vibrios from the environment. Proc. Natl. Acad. Sci. USA **97:**10231–10235.
54. **Overbeek, R., T. Begley, R. M. Butler, J. V. Choudhuri, H. Y. Chuang, M. Cohoon, V. de Crecy-Lagard, N. Diaz, T. Disz, R. Edwards, M. Fonstein, E. D. Frank, S. Gerdes, E. M. Glass, A. Goesmann, A. Hanson, D. Iwata-Reuyl, R. Jensen, N. Jamshidi, L. Krause, M. Kubal, N. Larsen, B. Linke, A. C. McHardy, F. Meyer, H. Neuweger, G. Olsen, R. Olson, A. Osterman, V. Portnoy, G. D. Pusch, D. A. Rodionov, C. Ruckert, J. Steiner, R. Stevens, I. Thiele, O. Vassieva, Y. Ye, O. Zagnitko, and V. Vonstein.** 2005. The subsystems approach to genome annotation and its use in the project to annotate 1000 genomes. Nucleic Acids Res. **33:**5691–5702.
55. **Park, J. T., and T. Uehara.** 2008. How bacteria consume their own exoskeletons (turnover and recycling of cell wall peptidoglycan). Microbiol. Mol. Biol. Rev. **72:**211–227.
56. **Rosenthal, R. S.** 1979. Release of soluble peptidoglycan from growing gonococci: hexaminidase and amidase activities. Infect. Immun. **24:**869–878.
57. **Rosenthal, R. S., W. Nogami, B. T. Cookson, W. E. Goldman, and W. J. Folkening.** 1987. Major fragment of soluble peptidoglycan released from growing *Bordetella pertussis* is tracheal cytotoxin. Infect. Immun. **55:**2117–2120.
58. **Ruby, E. G., and L. M. Asato.** 1993. Growth and flagellation of *Vibrio fischeri* during initiation of the sepiolid squid light organ symbiosis. Arch. Microbiol. **159:**160–167.
59. **Ruby, E. G., M. Urbanowski, J. Campbell, A. Dunn, M. Faini, R. Gunsalus, P. Lostroh, C. Lupp, J. McCann, D. Millikan, A. Schaefer, E. Stabb, A. Stevens, K. Visick, C. Whistler, and E. P. Greenberg.** 2005. Complete genome sequence of *Vibrio fischeri*: a symbiotic bacterium with pathogenic congeners. Proc. Natl. Acad. Sci. USA **102:**3004–3009.
60. **Sambrook, J., E. F. Fritsch, and T. Maniatis.** 1989. Molecular cloning: a laboratory manual, 2nd ed., vol. 3. Cold Spring Harbor Laboratory Press, Cold Spring Harbor, NY.
61. **Scheurwater, E., C. W. Reid, and A. J. Clarke.** 2008. Lytic transglycosylases: bacterial space-making autolysins. Int. J. Biochem. Cell Biol. **40:**586–591.
62. **Sinha, R. K., and R. S. Rosenthal.** 1980. Release of soluble peptidoglycan from growing gonococci: demonstration of anhydro-muramyl-containing fragments. Infect. Immun. **29:**914–925.
63. **Stabb, E. V., K. A. Reich, and E. G. Ruby.** 2001. *Vibrio fischeri* genes *hvnA* and *hvnB* encode secreted NAD^+-glycohydrolases. J. Bacteriol. **183:**309–317.
64. **Stabb, E. V., and E. G. Ruby.** 2003. Contribution of *pilA* to competitive colonization of the squid *Euprymna scolopes* by *Vibrio fischeri*. Appl. Environ. Microbiol. **69:**820–826.
65. **Stabb, E. V., and E. G. Ruby.** 2002. RP4-based plasmids for conjugation between *Escherichia coli* and members of the Vibrionaceae. Methods Enzymol. **358:**413–426.
66. **Tamura, K., J. Dudley, M. Nei, and S. Kumar.** 2007. MEGA4: Molecular Evolutionary Genetics Analysis (MEGA) software version 4.0. Mol. Biol. Evol. **24:**1596–1599.
67. **Templin, M. F., A. Ursinus, and J. V. Höltje.** 1999. A defect in cell wall recycling triggers autolysis during the stationary growth phase of *Escherichia coli*. EMBO J. **18:**4108–4117.
68. **Uehara, T., and J. T. Park.** 2007. An anhydro-*N*-acetylmuramyl-L-alanine amidase with broad specificity tethered to the outer membrane of *Escherichia coli*. J. Bacteriol. **189:**5634–5641.
69. **Vezzi, A., S. Campanaro, M. D'Angelo, F. Simonato, N. Vitulo, F. M. Lauro, A. Cestaro, G. Malacrida, B. Simionati, N. Cannata, C. Romualdi, D. H. Bartlett, and G. Valle.** 2005. Life at depth: *Photobacterium profundum* genome sequence and expression analysis. Science **307:**1459–1461.
70. **Visick, K. L., J. Foster, J. Doino, M. McFall-Ngai, and E. G. Ruby.** 2000. *Vibrio fischeri lux* genes play an important role in colonization and development of the host light organ. J. Bacteriol. **182:**4578–4586.
71. **Visick, K. L., T. M. O'Shea, A. H. Klein, K. Geszvain, and A. J. Wolfe.** 2007. The sugar phosphotransferase system of *Vibrio fischeri* inhibits both motility and bioluminescence. J. Bacteriol. **189:**2571–2574.
72. **Vollmer, W., B. Joris, P. Charlier, and S. Foster.** 2008. Bacterial peptidoglycan (murein) hydrolases. FEMS Microbiol. Rev. **32:**259–286.
73. **Whistler, C. A., T. A. Koropatnick, A. Pollack, M. J. McFall-Ngai, and E. G. Ruby.** 2007. The GacA global regulator of *Vibrio fischeri* is required for normal host tissue responses that limit subsequent bacterial colonization. Cell. Microbiol. **9:**766–778.
74. **Whistler, C. A., and E. G. Ruby.** 2003. GacA regulates symbiotic colonization traits of *Vibrio fischeri* and facilitates a beneficial association with an animal host. J. Bacteriol. **185:**7202–7212.
75. **Yip, E. S., K. Geszvain, C. R. DeLoney-Marino, and K. L. Visick.** 2006. The symbiosis regulator *rscS* controls the *syp* gene locus, biofilm formation and symbiotic aggregation by *Vibrio fischeri*. Mol. Microbiol. **62:**1586–1600.